21p

THE EVALUATION OF SEVERAL COMMERCIALLY AVAILABLE ACCELEROMETERS

By Tom D. Finley

NASA Langley Research Center
Langley Station, Hampton, Va.

Presented at I.R.I.G. Fourth Transducer Workshop

Wright-Patterson AFB, Cleveland, Ohio
June 18-19, 1964

THE EVALUATION OF SEVERAL COMMERCIALLY AVAILABLE ACCELEROMETERS

By Tom D. Finley*
NASA Langley Research Center

Ten years of experience in calibrating accelerometers at Langley Research Center has revealed that often these instruments will not meet claims as advertised and that many factors affecting performance are not included in manufacturers' specifications. This has led to the accelerometer evaluation program presently underway at Langley. The purpose of the program is to aid in the effort to obtain more accurate and more reliable data from commercially available accelerometers.

22182 ABST

This paper discloses some of the problems encountered during accelerometer calibrations and discusses some of the techniques, in particular the continuous plot, which can be used to reveal instrument errors.

The first and major portion of this paper deals with one accelerometer of the servo type, Brand A; the second part is a collection of findings on accelerometers of different types. (The names of the manufacturers are withheld to avoid prejudice and allow the reader to look objectively at the problems discussed.)

I. Brand A

Brand A servo accelerometer was the first brand to be tested in our present accelerometer evaluation program. Evaluation of this accelerometer is still incomplete. It was chosen for our first evaluation because its design features as advertised indicated conformance to Langley Research Center telemetry and general application requirements, and because this brand of accelerometer was in frequent use in ground facilities and in space payloads. Figure 1 is a sketch of a cutaway view of Brand A and figure 2 is an operational block diagram. These figures will be helpful in a discussion of the instrument's operation. The flexure-supported seismic mass, which houses two capacitor plates, moves with respect to the stationary capacitor plates when subjected to acceleration. This motion unbalances a capacitance bridge (made up of the sensing capacitors and two fixed capacitors which are not shown) and the bridge output current flows in the force coil of the seismic mass. This force coil current in the magnetic field provides the restraining force which servo controls the position of the mass. This current also flows through a range resistor which can be selected to vary the range of the accelerometer.

1. The nonlinearity and hysteresis were determined using three methods. Each method had limitations but it was felt that all would help to better determine these characteristics.

(a) The results of the first method are shown in figure 3. The instrument was ranged for ±0.5g full scale and positioned on a dividing

---

*Aerospace Technologist.

[redacted]

head. The output was read directly on a differential voltmeter. The upper graph is a direct plot of the accelerometer's output versus the input acceleration obtained by tilting in the field of gravity. The second graph represents the deviation of the output from a best straight line. With this method it was determined that the nonlinearity was approximately 0.04 percent full scale and the hysteresis was 0.01 percent full scale.

(b) The second method employed self-test or current insertion (fig. 4). The plot shows the error between the output voltage of the accelerometer (ranged at ±3g) and the voltage across a resistor in the current insertion circuit. (The force simulating acceleration was obtained by passing a current through a compensating coil wound on the same core as the forcer coil.) This method indicated approximately 0.01-percent full-scale nonlinearity and 0.01-percent full-scale hysteresis.

(c) The third method used was the error plot technique in which two similar accelerometers (ranged at ±50g) were accelerated simultaneously on a centrifuge and the difference in the outputs of the two instruments was plotted continuously on an X-Y plotter. The plot in figure 5 shows the results obtained using this method and indicates that the difference in linearity of the two instruments was 0.015 percent full scale and the hysteresis difference between the two accelerometers was 0.005 percent full scale. Thus all three methods indicate hysteresis of 0.01 percent or less and nonlinearity of 0.04 percent or less.

2. The effects of temperature on the scale factor of the accelerometer were investigated by performing ±1g calibrations on the instrument at -28° F, 94° F, and 180° F. The scale factor change for the 208° F change was only 0.001 percent/°F (manufacturer claimed 0.02 percent/°F). The zero shift of four Brand A accelerometers is plotted in figure 6. It should be noted that one of these instruments ranged for ±50g shifted 0.1 percent full scale which would be 10 percent full scale when ranged for $\pm\frac{1}{2}$ g.

3. The dynamic characteristics of the accelerometer are a function of the load resistor (fig. 7). The curves show that as the load resistor increases (i.e., the range decreases) the natural frequency decreases and the damping ratio increases. (The data shown are based on ±5-volt full-scale output.) Figure 8 shows the resulting change in response of the instrument when ranged for ±0.5g and when ranged for ±50g. In the latter case the response is flat within ±5 percent to 400 cps while in the former the flat response extends to only 10 cps. It should be noted that if less output is permissible (a smaller load resistor) the wider flat-frequency response can be maintained.

4. Damping stability - Tests were also performed on the accelerometer to determine the change in frequency response with temperature and vacuum. Figure 9 shows the accelerometer's frequency response under atmospheric pressure at 78° F, atmospheric pressure at 175° F, and 0.02 psia at 78° F. There was no change in response. This dynamic stability constitutes a notable advantage over many other types of instruments.

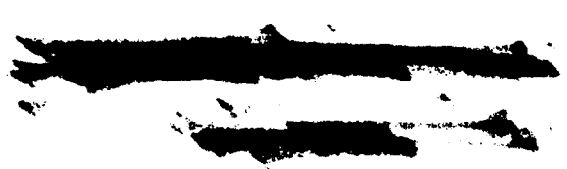

5. Damping technique - One unit was available for testing on which the hermetic seal had accidently been broken. The portion of damping force due to the air in the instrument was determined from the frequency response at pressures of 1 atmosphere and 1 mm Hg. (The manufacturer claimed that the instrument was electrically damped.) The results are shown in figure 10. Ranged ±50g, the accelerometer changed from 0.8 critical to almost zero damping with the removal of the air. Ranged at ±1g the accelerometer changed from 1.5 to 0.25 critical damping which indicated that, although there is a small amount of damping due to other factors, most of the damping developed was from the encased gas (or air).

6. The input voltage was one factor which affected the accelerometer's frequency response. The manufacturer rates the instrument at an input voltage of 28 volts d-c ±10 percent. Figure 11 shows the frequency response and natural frequency changes when one unit was calibrated at 26 volts, 28 volts, and 30 volts. Note that the response varied as much as 20 percent near the natural frequency. From tests on several other samples it was found that the magnitude of the change was greater on underdamped units.

7. The amplitude of the imposed dynamic acceleration also affects the frequency response of the accelerometer (fig. 12). The response of a ±50g instrument varied as much as 20 percent near the natural frequency when calibrated at 1 g and at 50g. Determination at 1 g and at 10g differed by less than 2 percent. The amplitude effects on dynamic response were accompanied by progressively greater distortion above about 20g. The peak value of the output waveform was only approximately 1.25 times the rms value when subjected to 50g sinusoidal vibration.

8. The problem of mounting resonances was investigated by plotting the instrument's response from 10 cps to 10 kc. On several Brand A accelerometers the response remained below 10 percent above 500 cps. On another unit the output increased to 5.6 times the input at 5700 cps (fig. 13).

9. The electrostatic attraction between the capacitor plates of the accelerometer can present a problem. When the instrument was ranged to $\pm\frac{1}{2}$g the servo loop gain was so low that when the power was applied to the accelerometer, the seismic mass would remain against one of the fixed capacitor plates. Under these conditions the output voltage would go to 13 volts and the instrument would remain inoperative until the mass was shaken loose or power was removed and applied while the instrument was in another position. The manufacturer suggests the use of zener diodes to remedy this problem.

10. Tests performed employing current insertion in the compensation coil provided an accurate measure of the variation in output current per g with a large change of range resistor, 500 to 50,000 ohms (±50g and ±0.5g, respectively). The difference between the output current and a fraction of the insertion current was plotted against the value of the inserted current (similar to fig 3). The inserted current simulated acceleration. Of the two units tested, the output current per g of one accelerometer increased 1 percent and the other decreased the same amount. Thus, for greater accuracy, range resistor changes on the accelerometer should be followed by calibrations or the accelerometer

should be calibrated originally with several range resistors to permit future range changes in the field.

11. The accelerometer's sensitivity to acoustic noise was in question because of the configuration of the seismic mass and the gas coupling. Acoustic noise from 20 to 2000 cps at levels of 120 to 140 dB was imposed on an accelerometer ranged ±5g and ranged ±50g. The effect was small and the data fell within the experimental error of the tests.

12. The scale factor change with input voltage variation was determined on several different ranges. With a ±10-percent change in the input voltage (tolerance given by the manufacturer) sensitivity of an accelerometer ranged at ±0.5g changed approximately 1 percent. The higher ranges were less affected.

13. Some preliminary life tests have been conducted on Brand A accelerometers. The units were subjected to a two-axis vibration of 8g to 10g peak and frequencies from 10 cps to 2000 cps. One unit suffered a failure after 70 hours. Another unit was placed in the environment and failed after 14 hours. In the final test in this series a sample of this accelerometer from a lot recently delivered to Langley was subjected to this environment for 1000 hours with no effect on performance.

II. The following is a collection of findings on accelerometers of different types:

Brand B Servo Accelerometer

The instrument was lightweight, 1.7 ounces, and relatively inexpensive. The sample tested was a ±1g unit with a full-scale output of ±7.5 volts. The unit was placed in a ±10g vibration field for 1000 hours, suffered no failures, and later repeated its original calibration. The frequency response was flat within ±15 percent to 170 cps. In terms of static response the linearity was 0.03 percent and the hysteresis 0.16 percent. One very serious effect occurred when the negative input voltage was reduced (the manufacturer recommends a ±15-volt d-c input power ±15 percent). When the negative voltage was reduced 15 percent the -g sensitivity decreased approximately 10 percent (fig. 14).

Brand C Servo Accelerometer

This ±3g unit had a 0- to 5-volt d-c output and a 28-volt d-c input. The unit was found to have flat frequency response ±2 percent to 120 cps and ±10 percent to 400 cps. The static calibration repeated within 0.1 percent after approximately 1000 hours in a 10g vibration field. There was a region near 300 cps where the output displayed noticeable distortion.

Brand D Servo Accelerometer

Brand D air-damped servo accelerometers, although much lighter and less temperature sensitive than the oil-damped units, had unusual dynamic characteristics. The frequency response dropped off and then rose in the region of the natural frequency. A very serious defect in the instrument was its fragile bearing structure. After the units were subjected to dynamic calibrations near

their natural frequency, the output waveforms were distorted (fig. 15). The manufacturer said that the bearings had been fractured and stated "We wish to stress to you . . . that we do not recommend high gain electrically damped units to be used for relatively high g vibration studies." It should be noted, however, that the failure occurred during a calibration within the amplitude and frequency range of the instrument as specified in the manufacturer's literature.

Brand E Strain-Gage Accelerometer

These liquid-damped unbonded strain-gage accelerometers are in wide use at Langley because of their size, weight, simplicity, and cost. Most of these units perform satisfactorily but many have displayed difficulties because of trash and gas bubbles in the damping fluid. Reproduced in figure 16 is an X-ray photograph of two transducers which plainly shows the presence of gas bubbles. Figure 17 shows continuous plots of a Brand E accelerometer output versus acceleration imposed on a centrifuge. The malfunction was repeatable and was caused by trash or debris in the damping fluid. It should be noted that these malfunctions would be very difficult to discover without the use of a continuous plot. Figure 18 represents a direct plot of the output of a Brand E accelerometer versus acceleration. These excursions were not repeatable and it is presumed that they are caused by a bubble in the fluid. Figure 19 shows a continuous plot of the frequency response of another Brand E accelerometer. As the plot was proceeding, the shaker was inverted, righted, and inverted again. The gas bubble thus passed over the seismic mass giving a changing response.

Conclusions

1. Accelerometer acceptance tests should include tests for the following characteristics:

(a) Distortion:

(1) Static - Discontinuities can result from trash and air bubbles in the damping fluid.

(2) Dynamic - Damaged bearings, air bubbles, and nonlinear damping can cause poor wave shapes or unstable frequency response.

(b) Damping Stability - The instrument should be calibrated under vacuum to determine if the seal is sufficient to maintain damping (either air or liquid).

(c) Resonances - The instrument's response should be continuously plotted to 10 kc or higher to disclose any mounting or spurious resonance.

(d) Scale factor vs. input voltage.

(e) Damping vs. input voltage.

(f) Damping vs. amplitude.

2. The following techniques can be used effectively to detect faults in accelerometers:

(a) X-rays of liquid-damped instruments.

(b) Continuous X-Y plotting (Dynamic and Static) - Many of the problems discussed in this paper would have been virtually impossible to detect without the use of this technique.

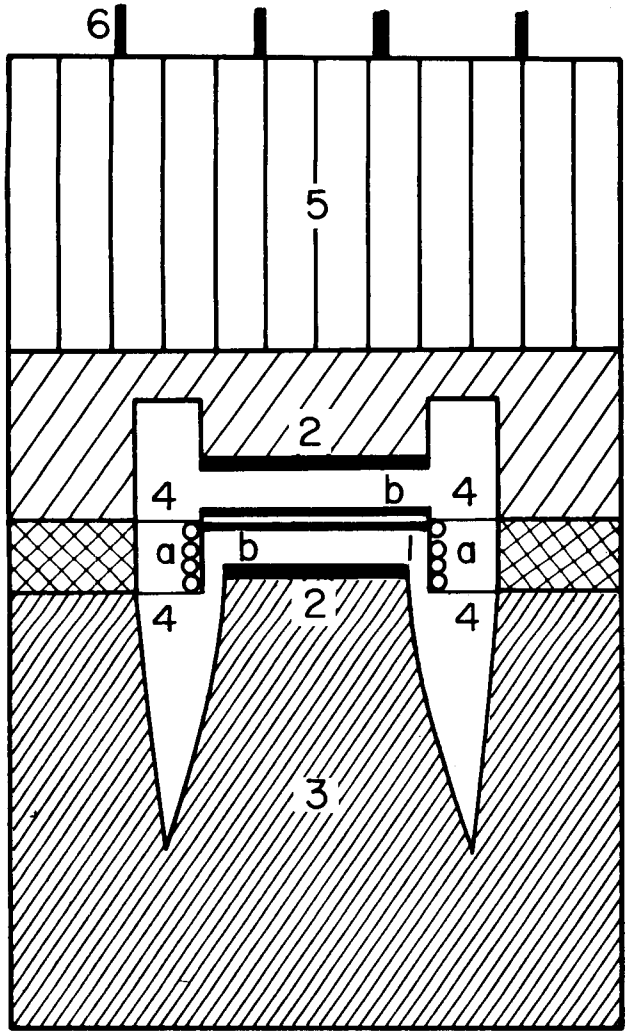

1. SEISMIC MASS
   a. FORCER COIL AND COMP. COIL
   b. MOVING PLATES
2. FIXED PLATES
3. MAGNET
4. FLEXURES
5. ELECTRONICS
6. EXTERNAL CONNECTIONS

NASA

Figure 1.- Brand A - Cutaway view.

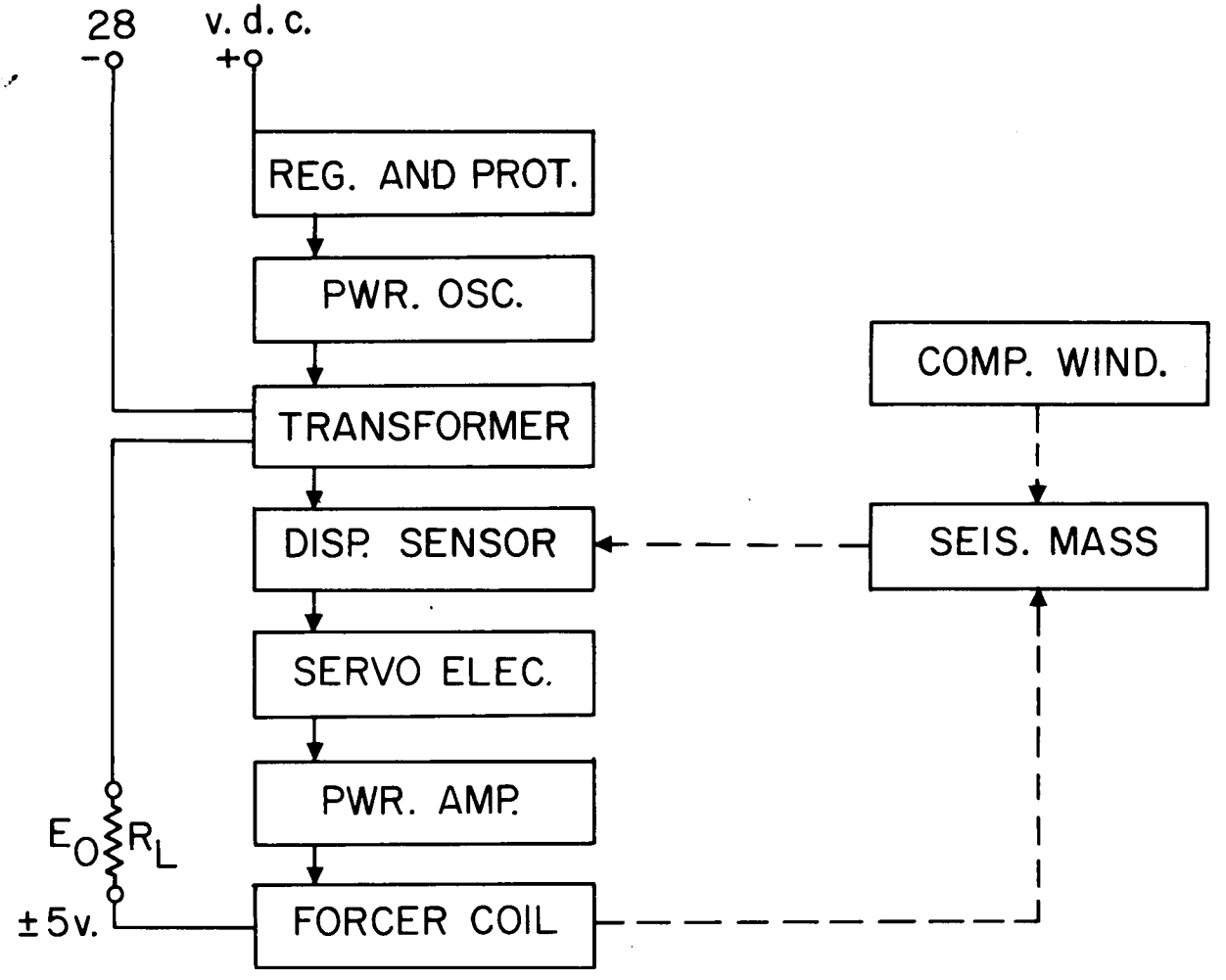

Figure 2.- Brand A - Operational block diagram.

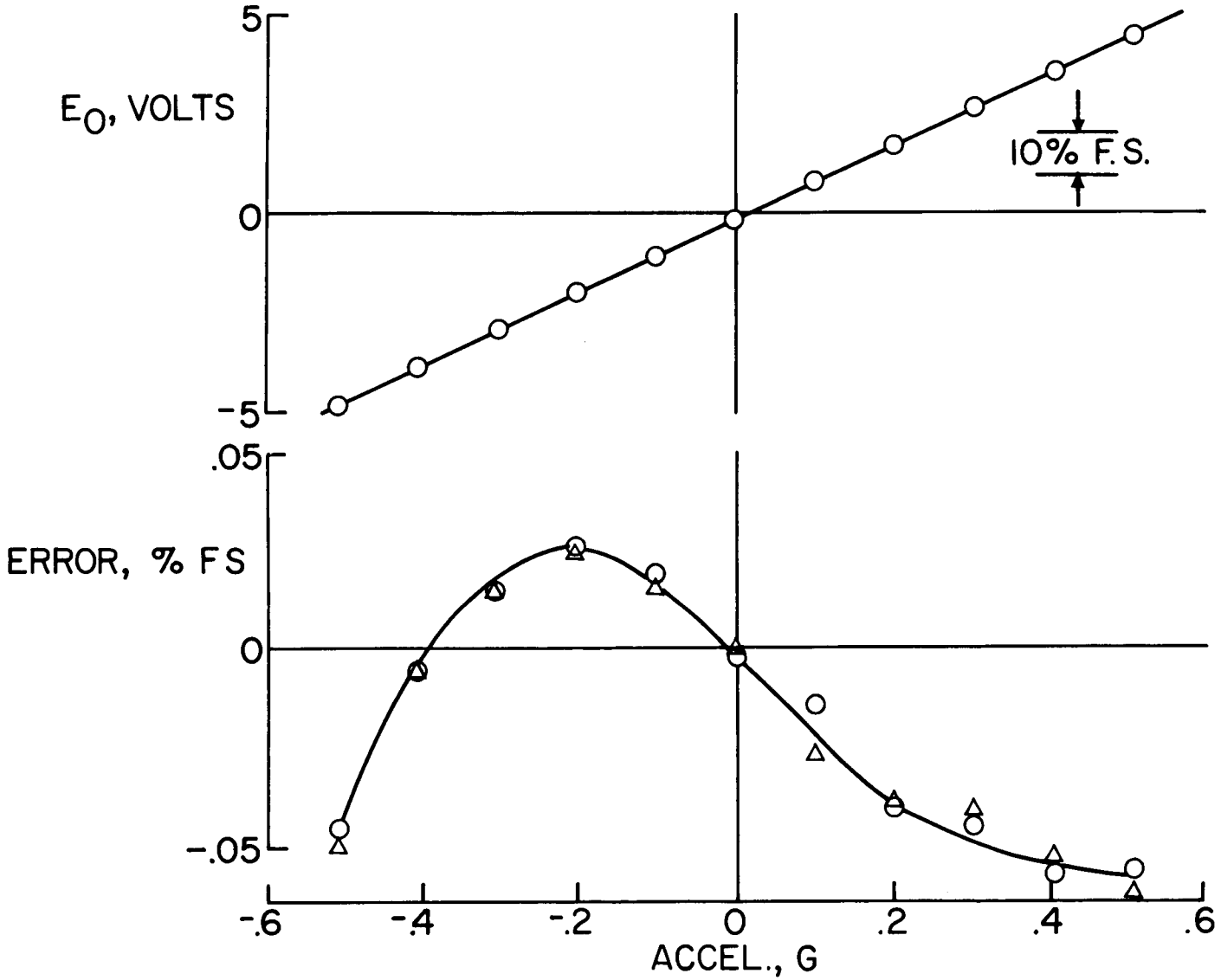

NASA

Figure 3.- Brand A - Nonlinearity and hysteresis, direct calibration.

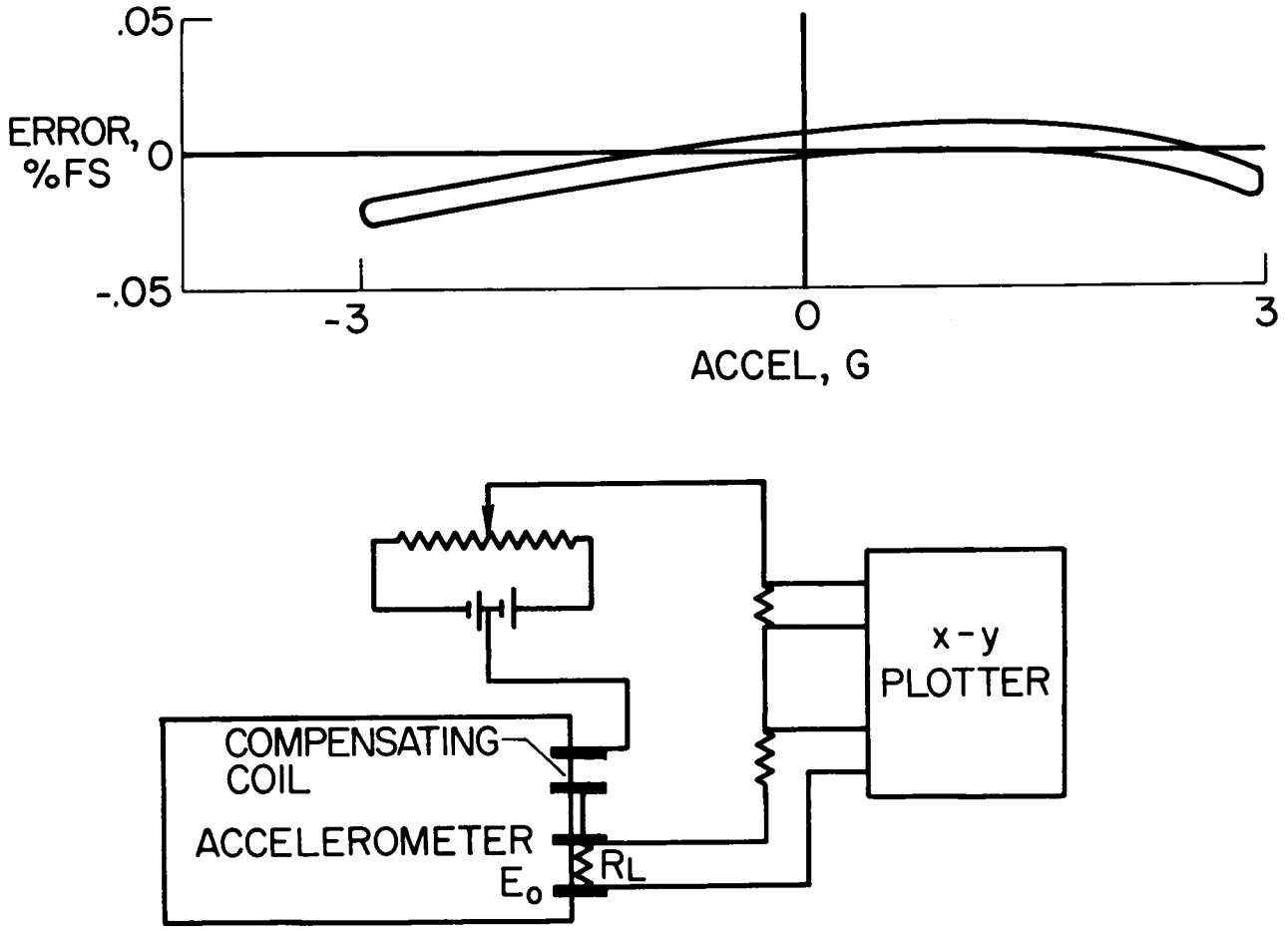

NASA

Figure 4.- Brand A - Nonlinearity and hysteresis, self test.

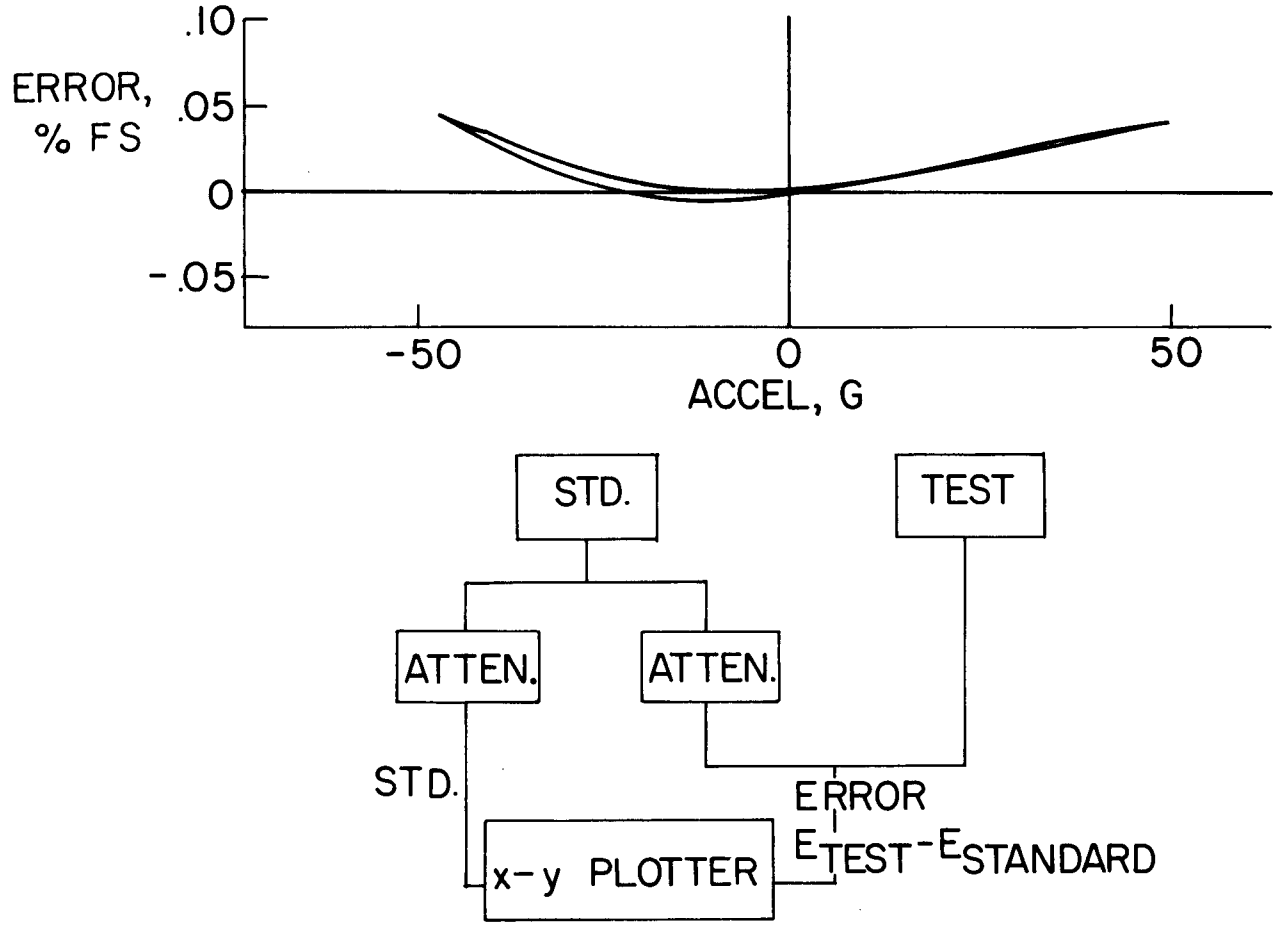

NASA

Figure 5.- Brand A - Nonlinearity and hysteresis, error plot.

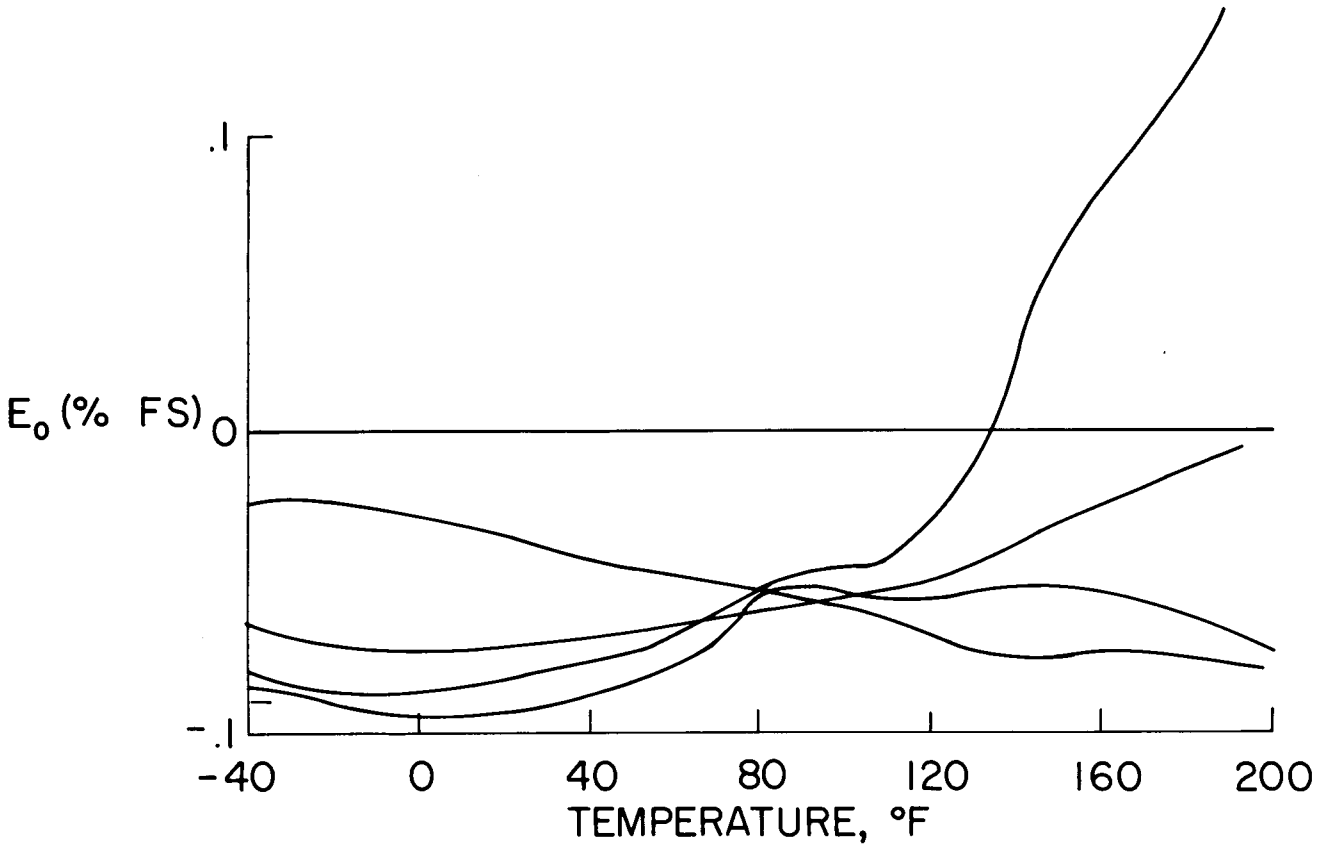

Figure 6.- Brand A - Temperature zero shift.

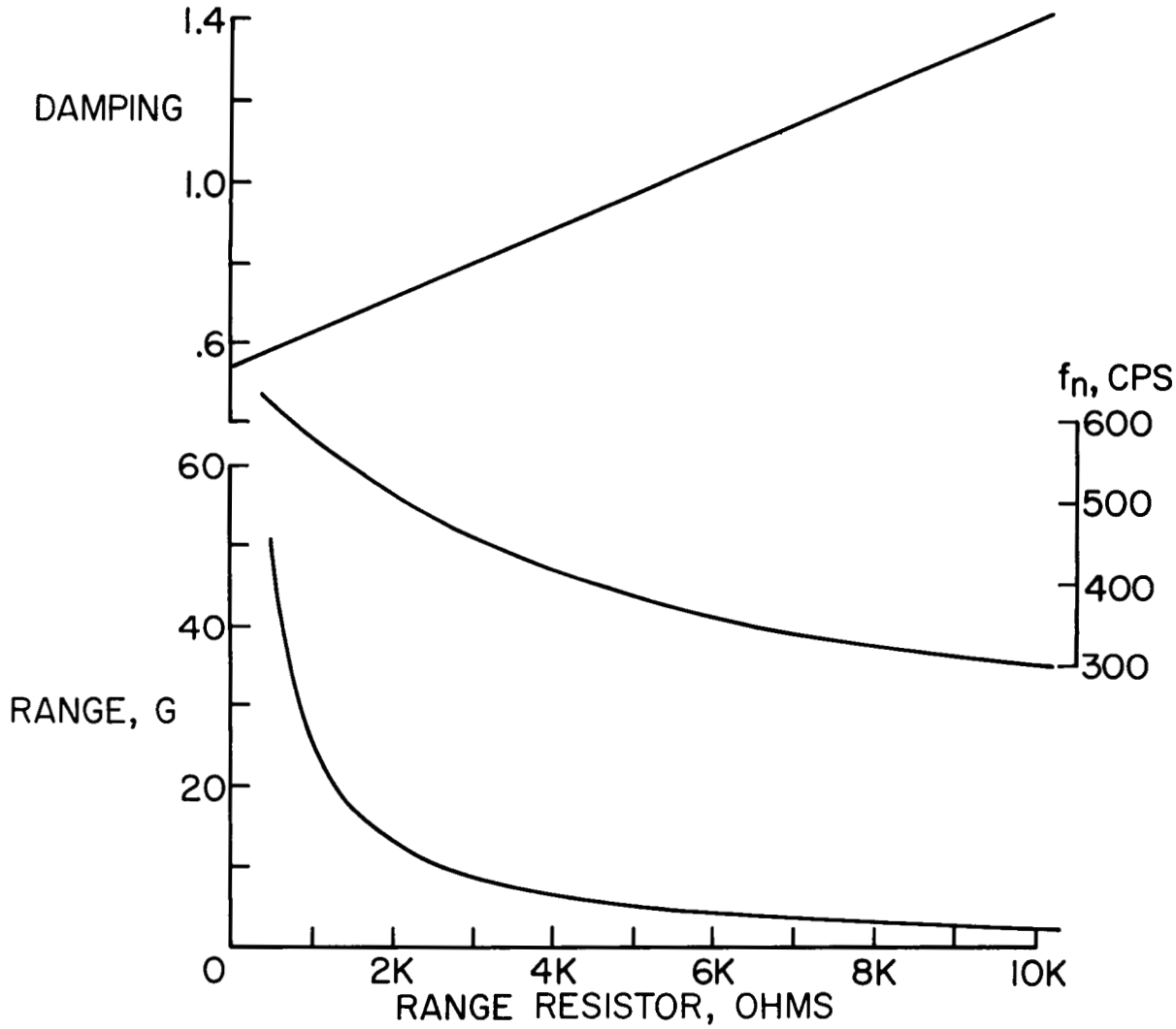

NASA

Figure 7.- Brand A - Dynamic characteristics.

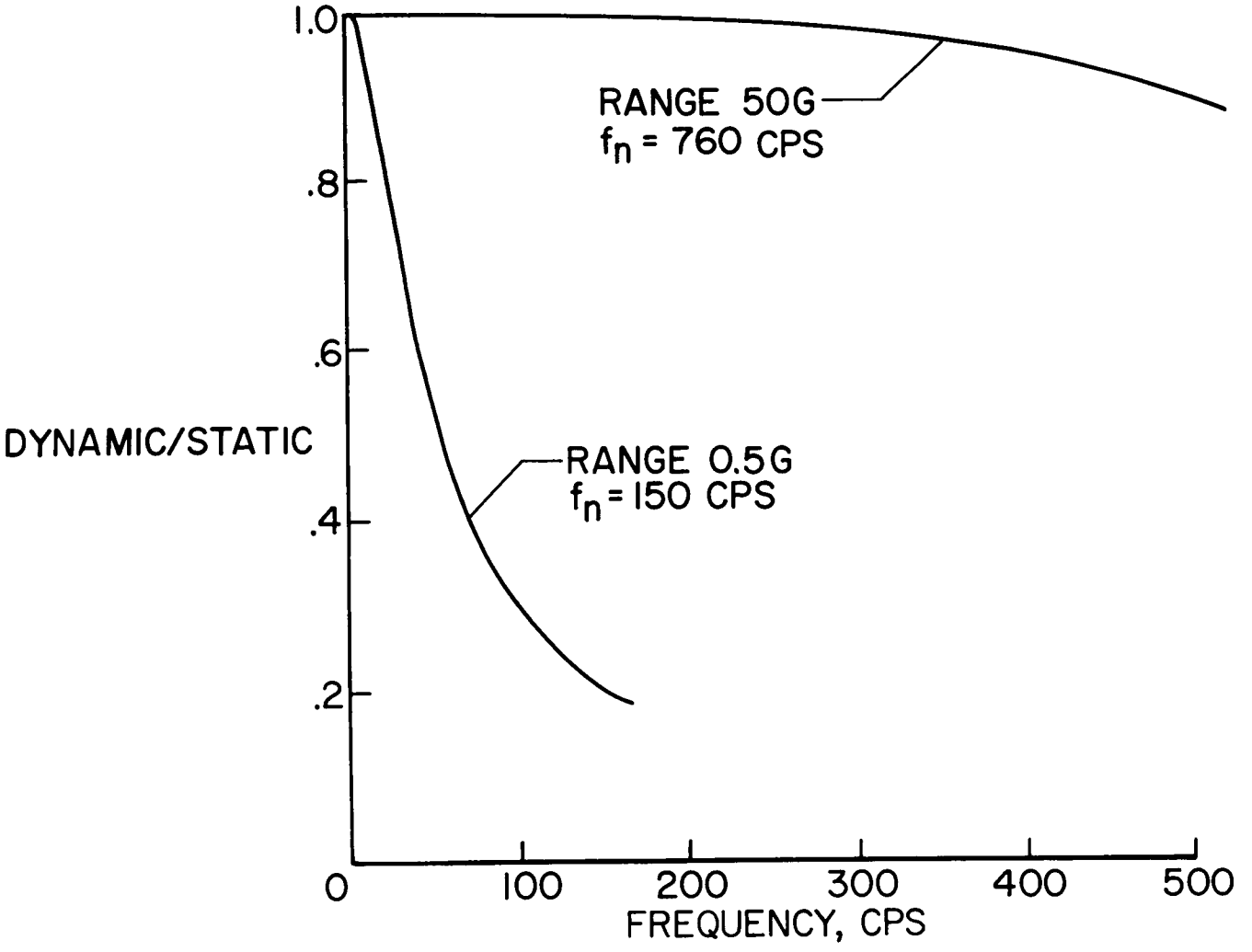

Figure 8.- Brand A - Frequency response at different ranges.

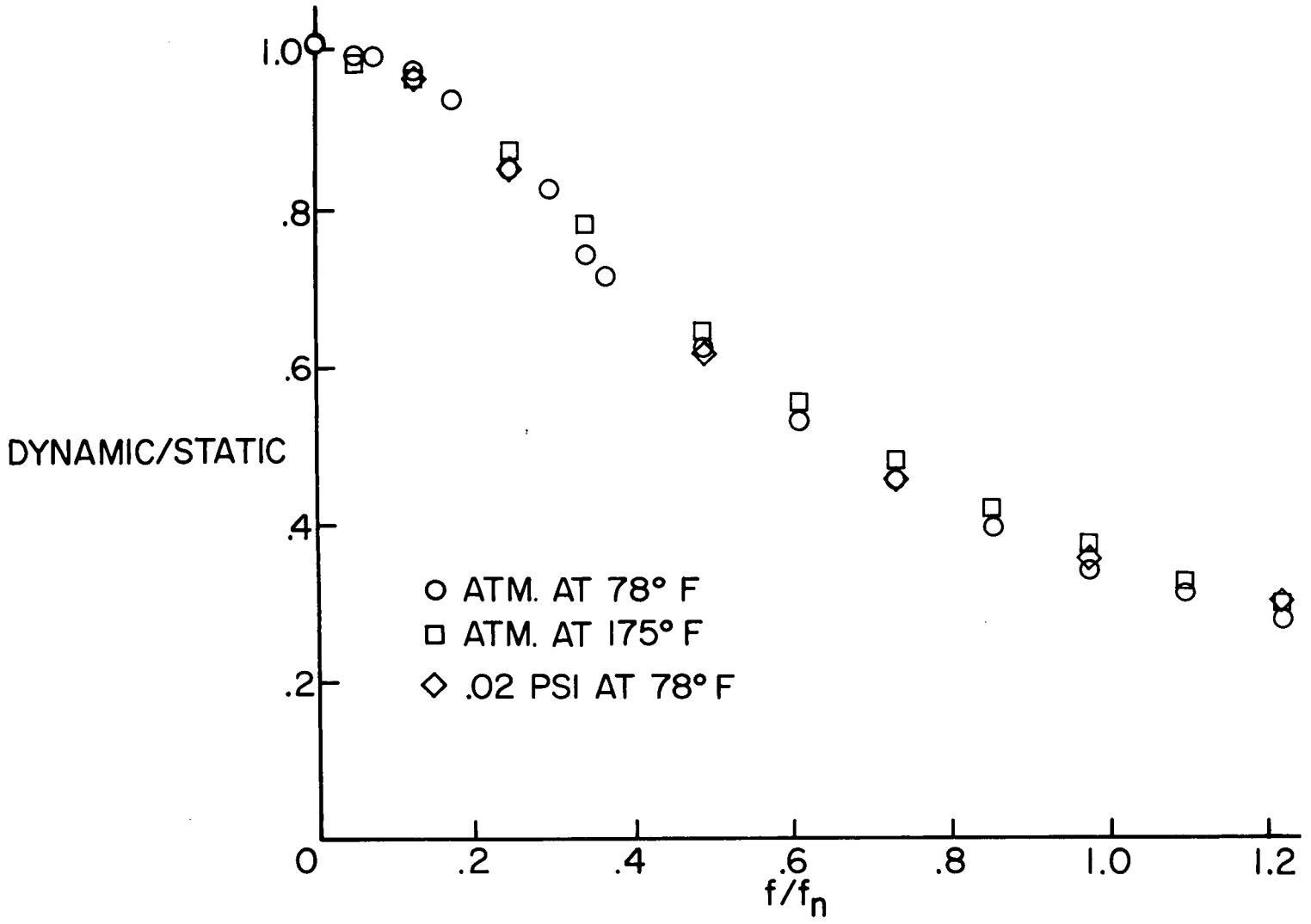

Figure 9.- Brand A - Damping stability.

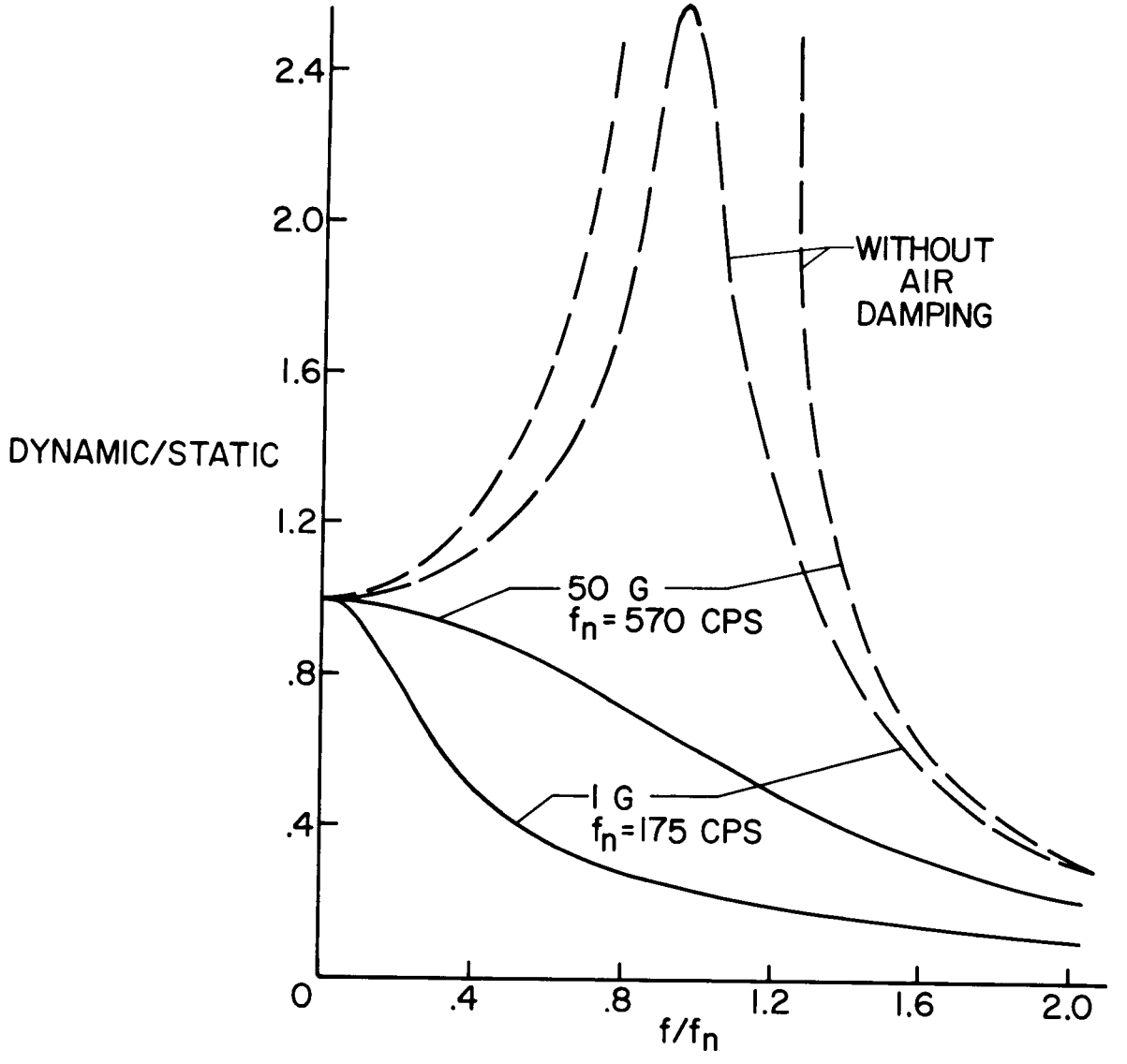

Figure 10.- Brand A - Damping technique.

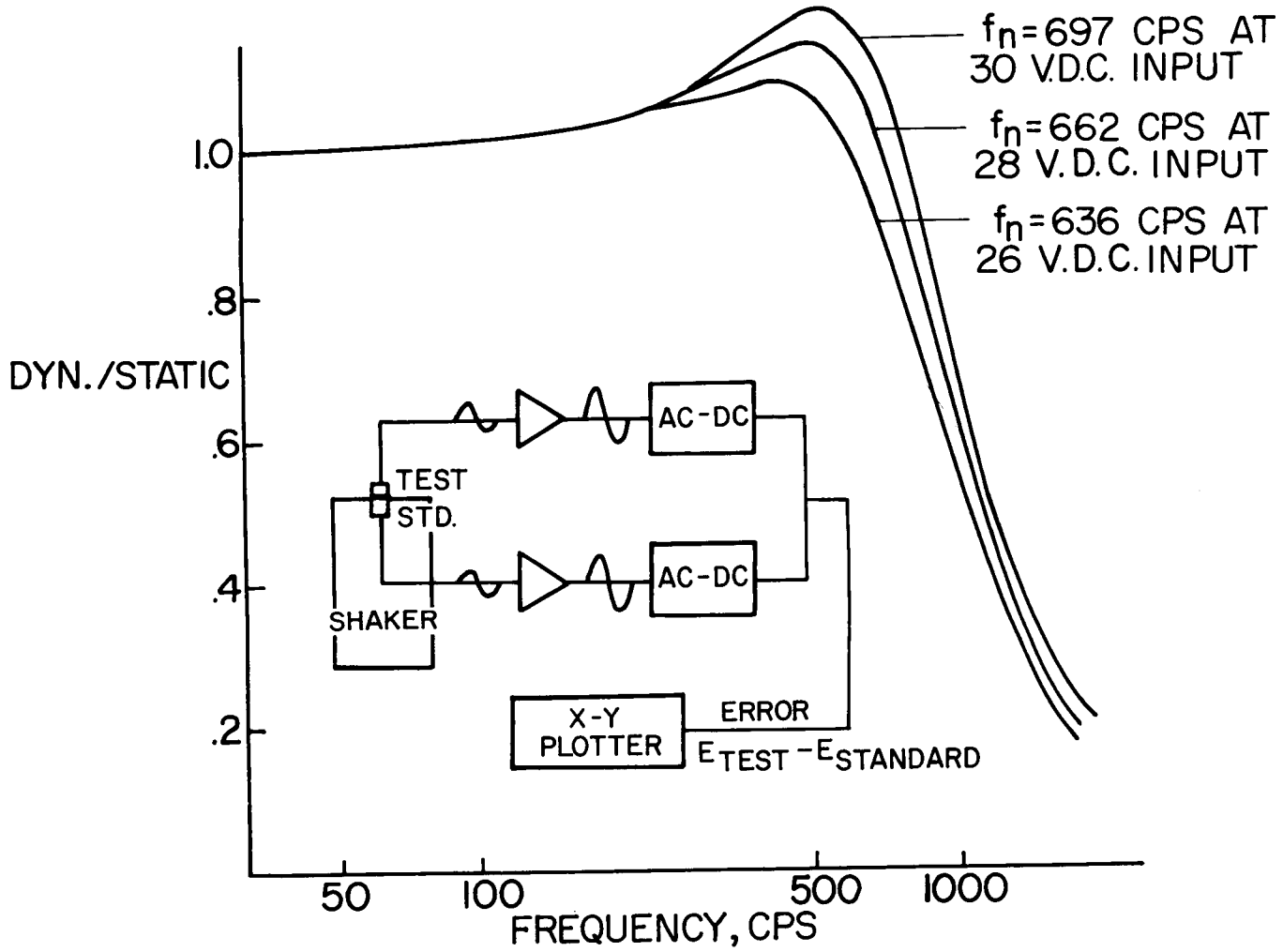

Figure 11.- Brand A - Damping versus input voltage.

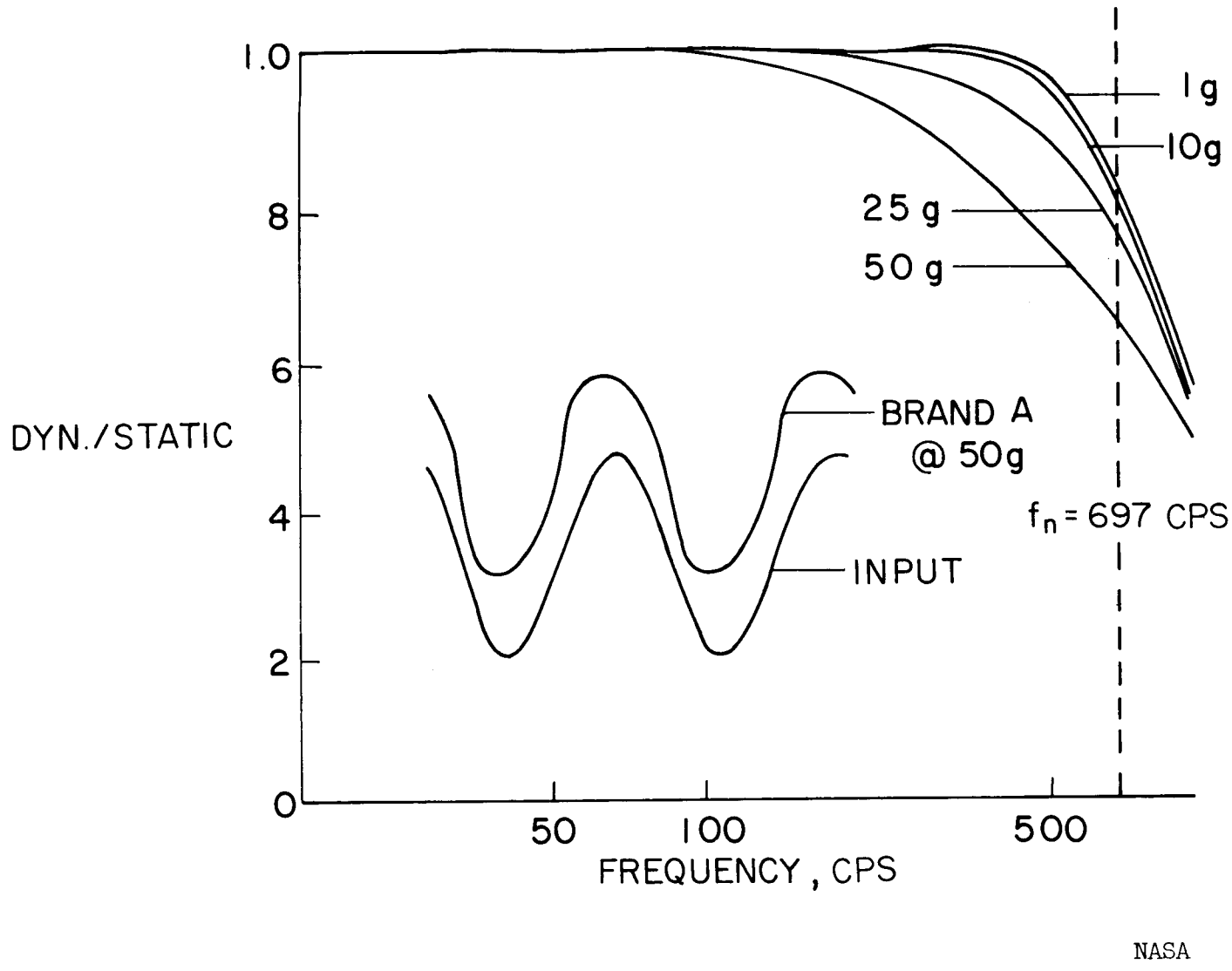

Figure 12.- Brand A - Damping versus amplitude.

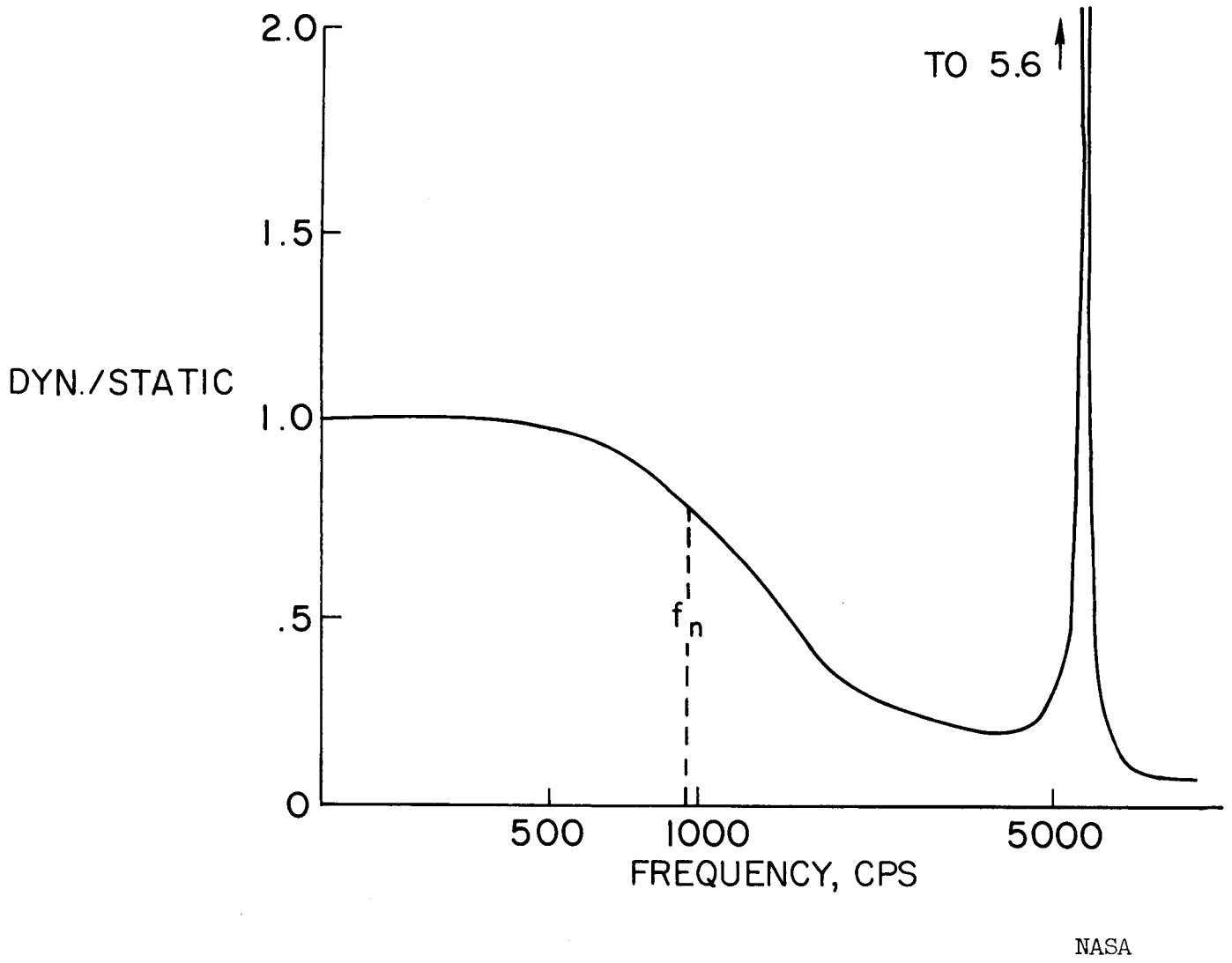

Figure 13.- Brand A - Mounting resonance.

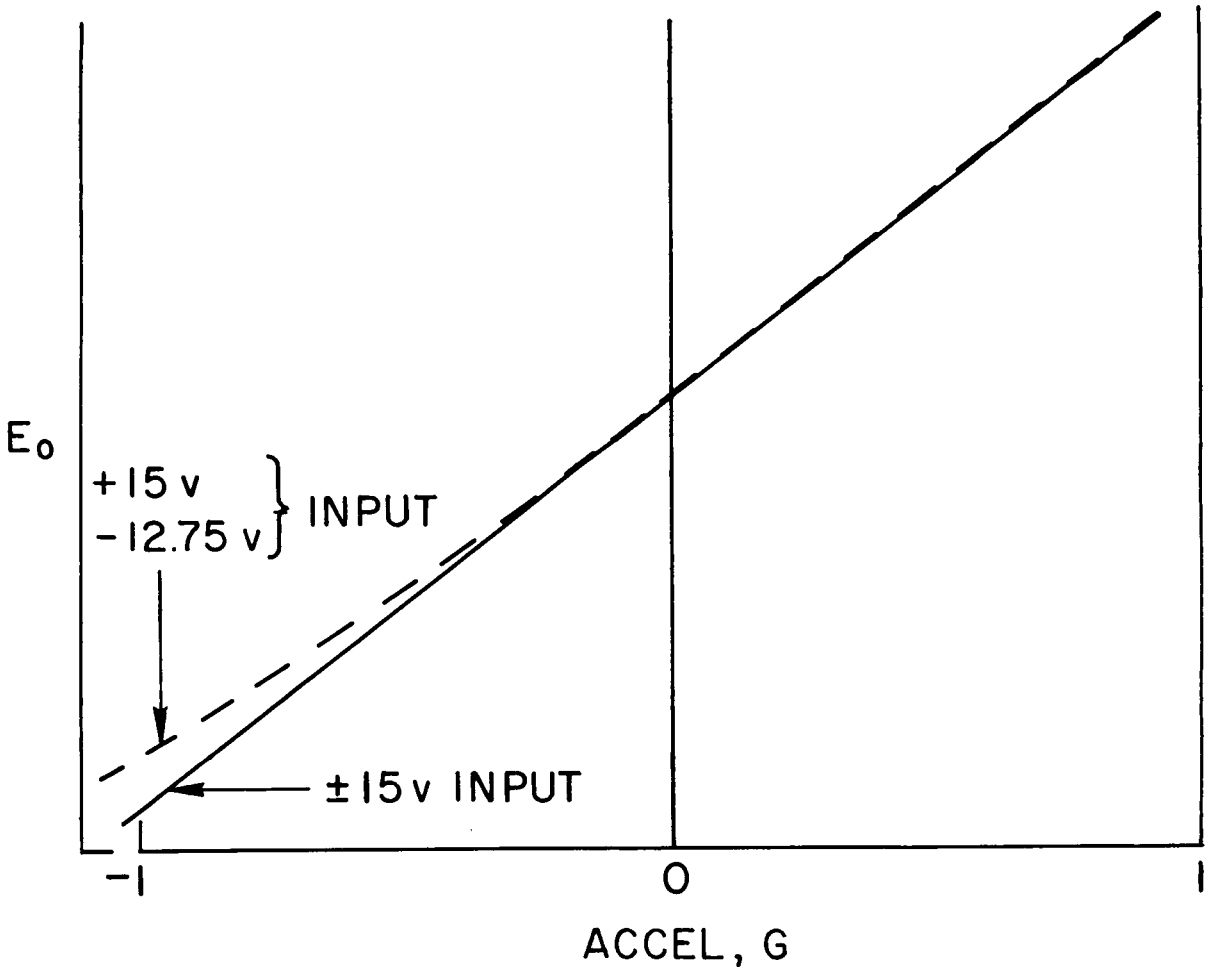

NASA

Figure 14.- Brand B - Sensitivity change with input voltage variations.

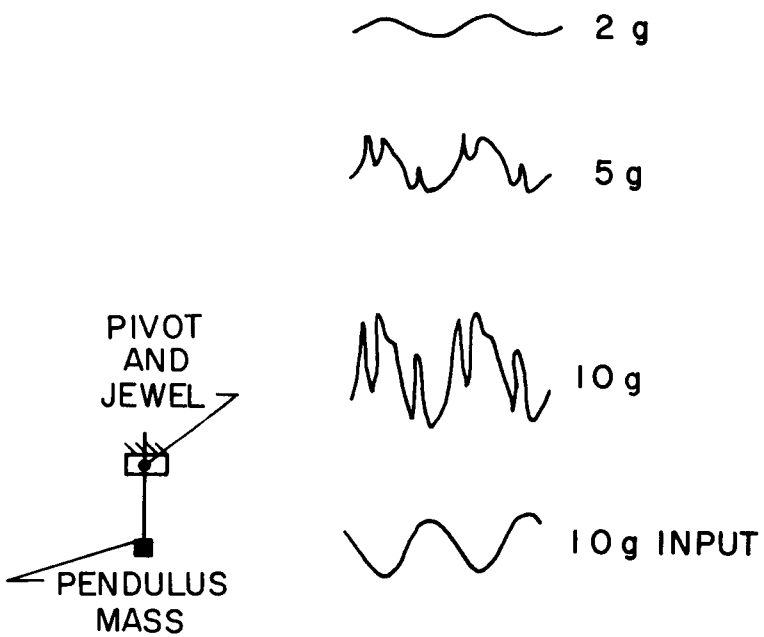

NASA

Figure 15.- Brand D- Dynamic distortion.

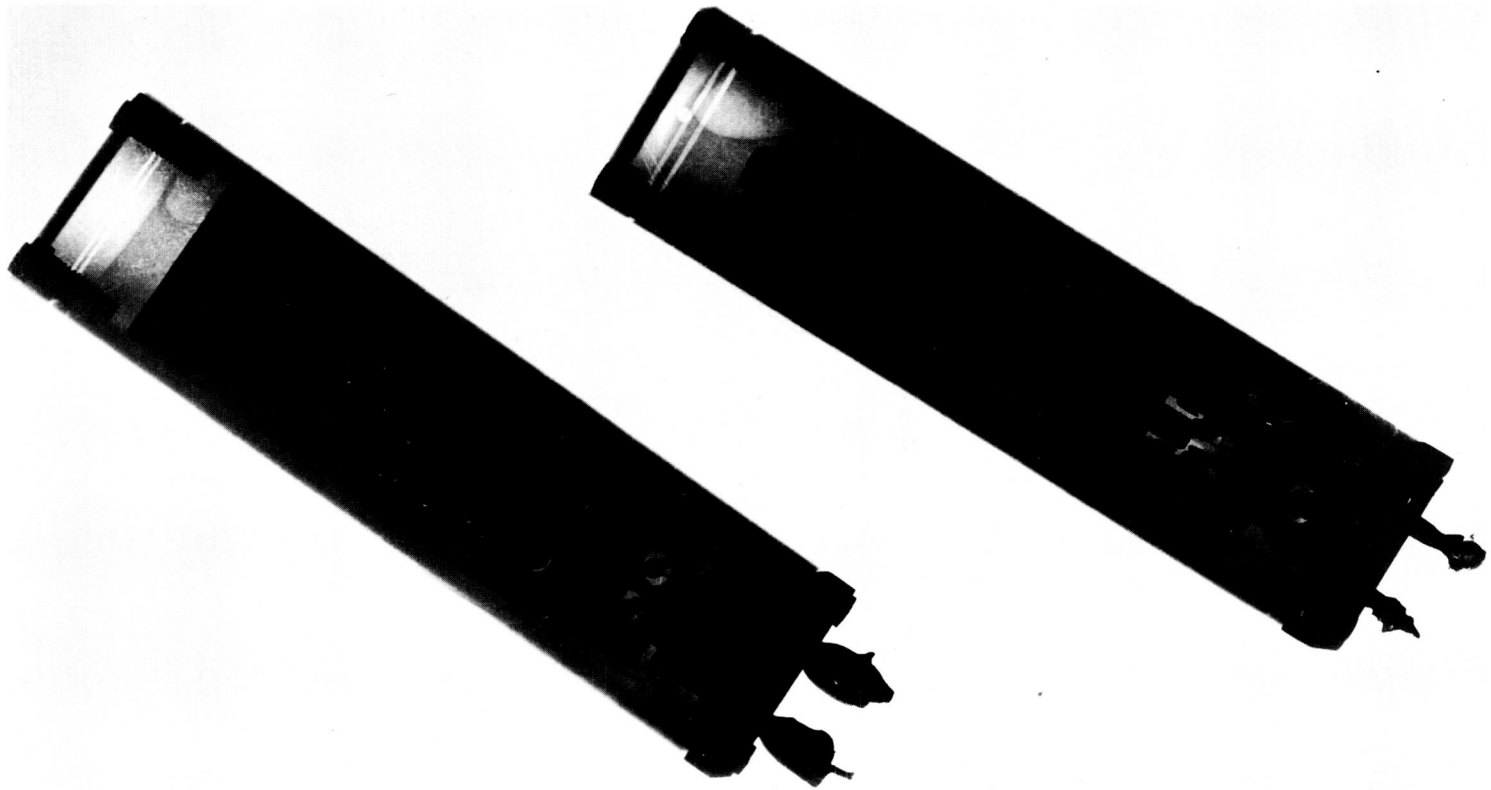

NASA

Figure 16.- Brand E - X-ray showing gas bubbles.

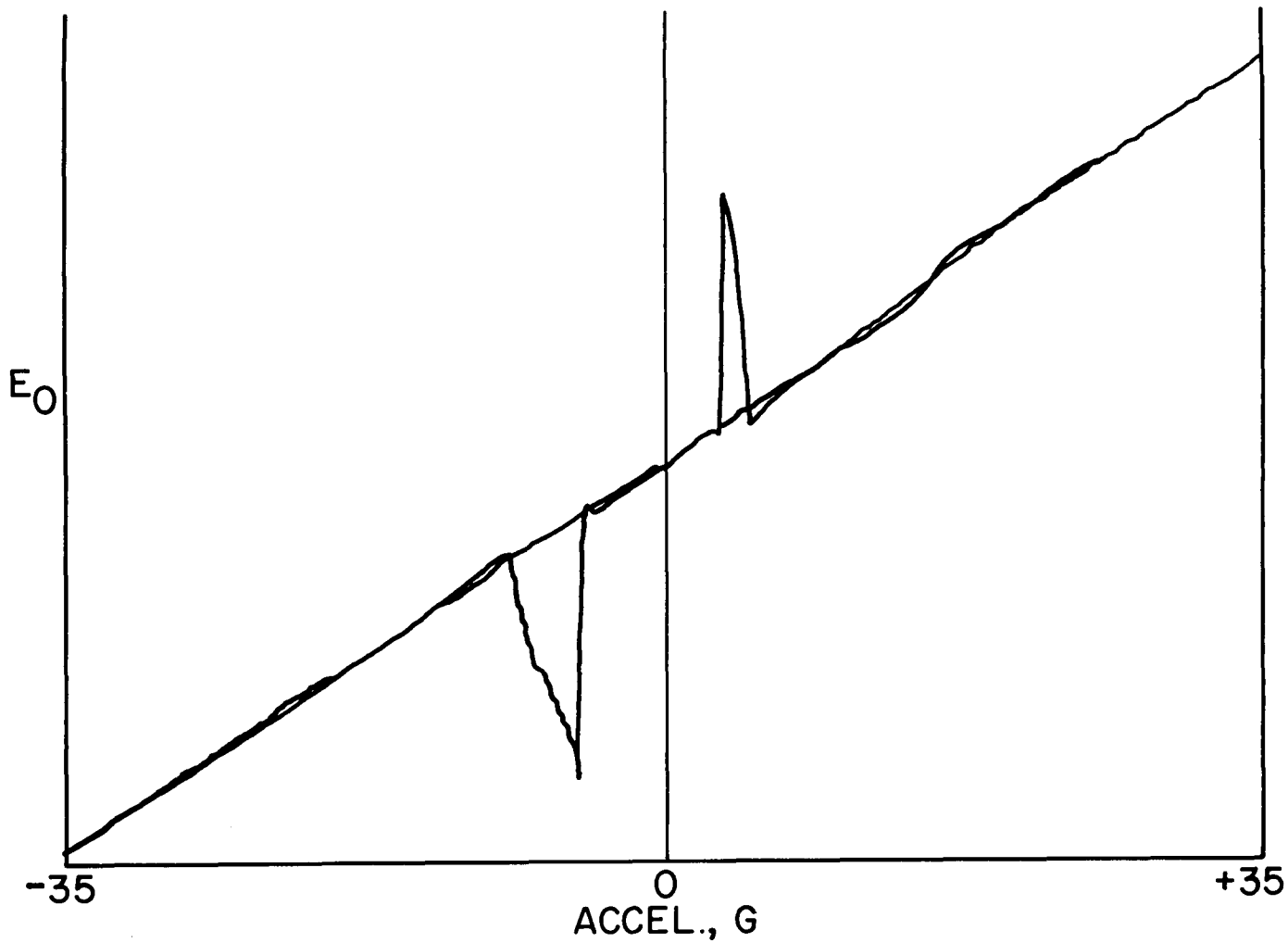

Figure 18.- Brand E - Continuous direct plot, static.

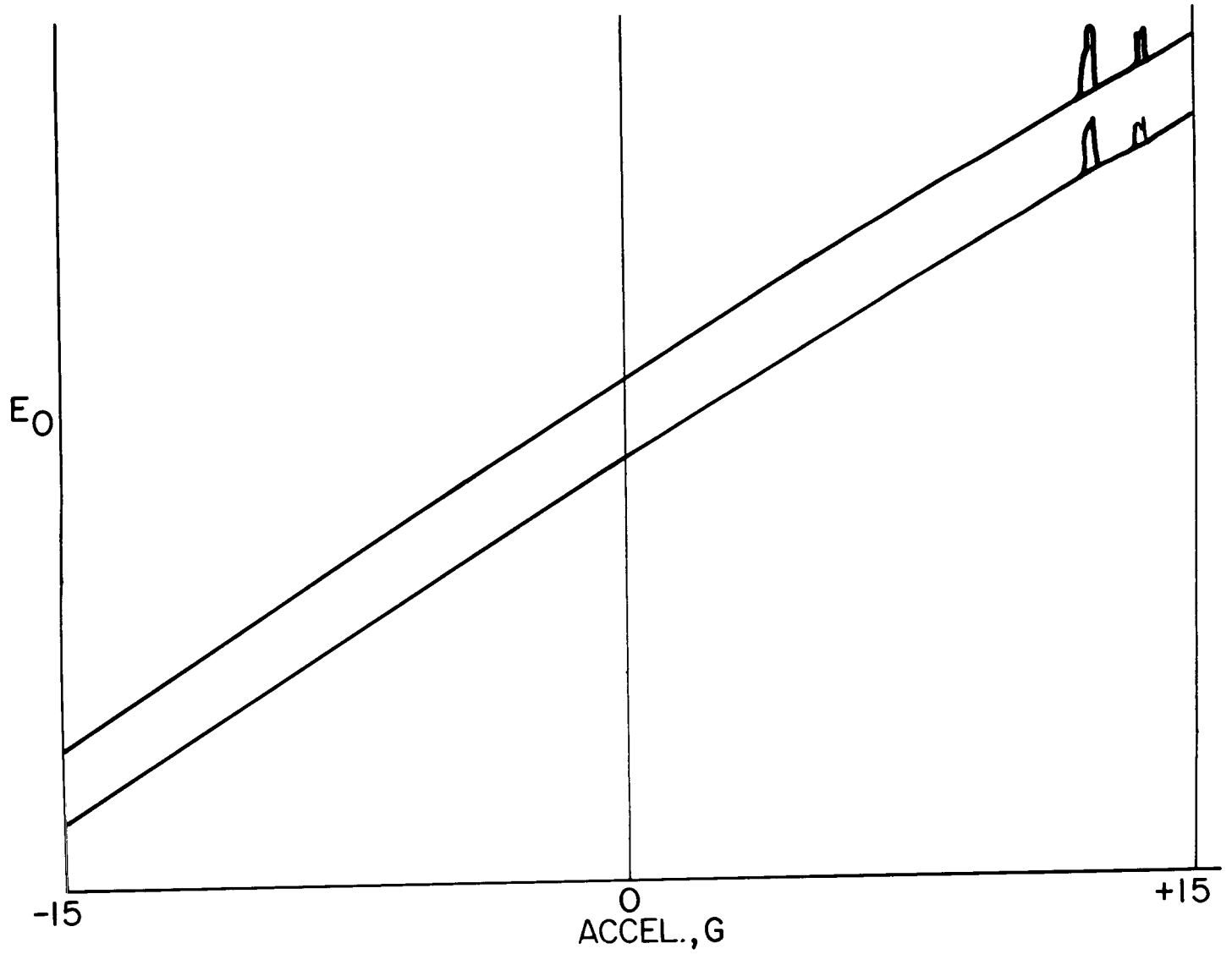

Figure 17.- Brand E - Continuous direct plot, static.

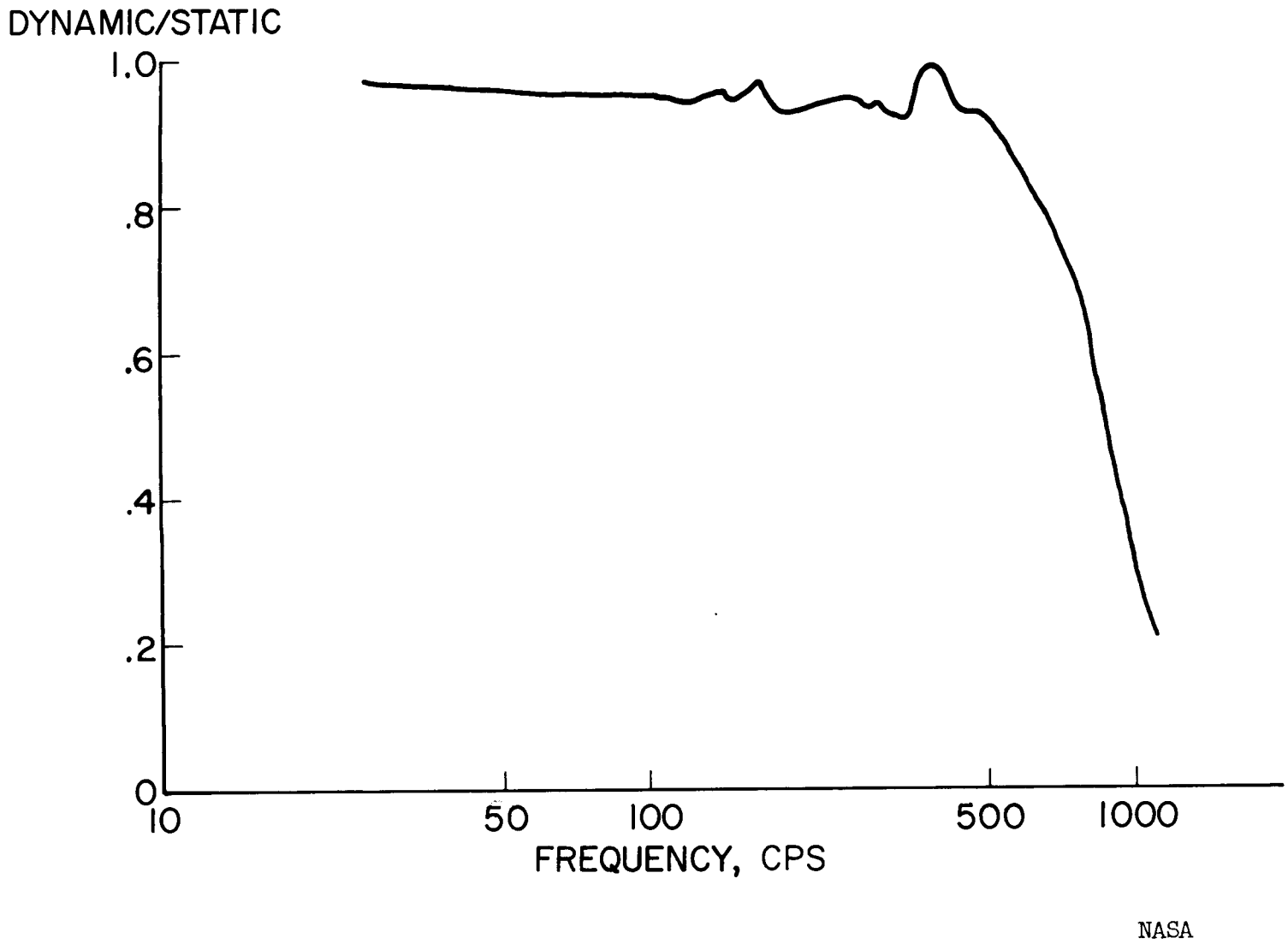

Figure 19.- Brand E - Continuous plot, dynamic.